

# Scission-point model predictions of fission-fragment mass and total kinetic energy distributions for $^{236}\text{U}$ and $^{252}\text{Cf}$

Fedor Ivanyuk<sup>1,a</sup>, Franz-Josef Hambsch<sup>2</sup>, and Nicolae Carjan<sup>3,4</sup>

<sup>1</sup> Institute for Nuclear Research, Kiev, Ukraine

<sup>2</sup> European Commission, Joint Research Center, Directorate G, Geel, Belgium

<sup>3</sup> Joint Institute for Nuclear Research, Dubna, Moscow Region, Russia

<sup>4</sup> National Institute of Physics and Nuclear Engineering, “Horia Hulubei”, Bucharest, Romania

**Abstract.** The total deformation energy at the moment of the neck rupture for  $^{236}\text{U}$  and  $^{252}\text{Cf}$  is calculated using the Strutinsky’s prescription and nuclear shapes described in terms of Cassinian ovals generalized by the inclusion of four additional shape parameters:  $\alpha_1$ ,  $\alpha_2$ ,  $\alpha_3$ , and  $\alpha_4$ . The corresponding fragment-mass distributions are estimated supposing that each point in the deformation space is occupied according to a canonical distribution. The energy distributions of fission fragments are calculated assuming the point-charge approximation for the Coulomb interaction of fission fragments. Finally, an alternative definition of the nuclear scission point configuration relying on the minimization of liquid drop energy (optimal shape method) is used. Both definitions lead, for these two nuclei, to a reasonably good agreement with the experimental data.

## 1. Introduction

We assume that the scission process (from the beginning of the neck rupture till the total absorption of the neck stubs by the fragments) is extremely fast [1]. During this transition the mass division is frozen and the distance between centers of mass of future fragments stays practically unchanged. So, the fission-fragment properties have to be estimated “just-before scission”, not when the fragments are already separated. Thus, the scission-point model [2] should be applied at this configuration in order to calculate the fission-fragment mass and total kinetic energy distributions.

Recently such a model was used for the calculations of distributions for the spontaneous fission of Fm, No, Rf and Sg isotopes [3]. In this work the pre-scission shapes were defined in terms of modified Cassinian ovals. Besides the elongation parameter  $\alpha$  the other two most relevant shape parameters were included:  $\alpha_1$  (the mass asymmetry) and  $\alpha_4$  (the neck radius). In addition the minimization of the deformation energy with respect to  $\alpha_6$  was performed.

This improved scission model described successfully the observed transition from asymmetric to symmetric fission that occurs, for the above mentioned isotopes, when the mass of the fissioning nucleus increases. It is therefore desirable to apply the model also to actinide nuclei which are of greater interest to nuclear data. In this study we estimate the fission fragment properties for the most important of them:  $^{235}\text{U}(n_{th}, f)$  and  $^{252}\text{Cf}(sf)$ .

The formalism employed is described in Sect. 2, while the numerical results are presented in Sect. 3. In Sect. 4 an alternative definition of the nuclear shapes just before scission is presented and applied to the same observables. Section 5 contains the summary and the conclusions.

## 2. The shape parameterization

A convenient orthogonal system to describe the shape of a fissioning nucleus is the lemniscate coordinate system  $(R, x)$  [4]. In this parameterization some (scaled) cylindrical co-ordinates  $\{\bar{\rho}, \bar{z}\}$  are related to the lemniscate co-ordinates system  $\{R, x\}$  by the equations

$$\begin{aligned}\bar{\rho} &= \frac{1}{\sqrt{2}} \sqrt{p(x) - R^2(2x^2 - 1) - s}, \\ \bar{z} &= \frac{\text{sign}(x)}{\sqrt{2}} \sqrt{p(x) + R^2(2x^2 - 1) + s}, \\ p^2(x) &\equiv R^4 + 2sR^2(2x^2 - 1) + s^2, \\ 0 &\leq R \leq \infty, -1 \leq x \leq 1.\end{aligned}\quad (1)$$

The basic lines  $R(x) = \text{const}$  represent a sequence of shapes (Cassinian ovals) that are surprisingly close to the sequence of shapes of a fissioning nucleus.

In (1)  $s \equiv \varepsilon R_0^2$  is the squared distance between the focus of Cassinian ovals and the origin of coordinates.  $R_0$  is the radius of the spherical nucleus.

The deviation of the nuclear surface from Cassini ovals is defined by expansion of  $R(x)$  in series in Legendre polynomials  $P_n(x)$ ,

$$R(x) = R_0 \left[ 1 + \sum_n \alpha_n P_n(x) \right]. \quad (2)$$

The cylindrical co-ordinates  $\{\rho, z\}$  are related to  $\{\bar{\rho}, \bar{z}\}$  by

$$\rho \equiv \bar{\rho}/c, \quad z \equiv (\bar{z} - \bar{z}_{\text{cm}})/c, \quad (3)$$

where  $\bar{z}_{\text{cm}}$  is the  $z$ -coordinate of the center of mass of Cassini ovaloid (2) and the constant  $c$  is introduced in order

<sup>a</sup> e-mail: ivanyuk@kinr.kiev.ua

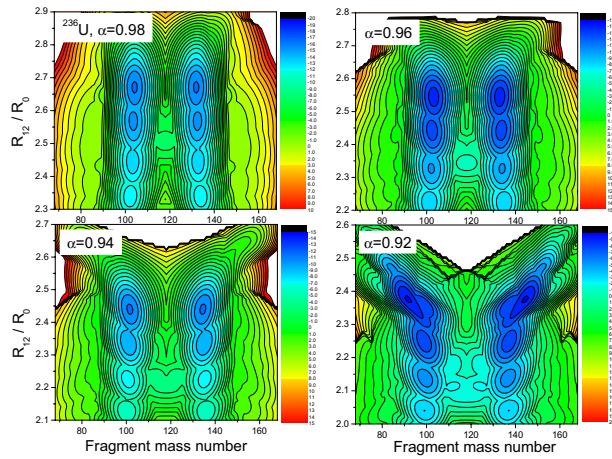


**Figure 1.** The deformation energy of  $^{236}\text{U}$  as a function of the mass asymmetry and elongation  $R_{12}$  for four fixed values of the deformation parameter  $\alpha$ .

to insure that the volume inside surface (2) is equal to the volume of the spherical nucleus.

Instead of the elongation parameter  $\varepsilon$ , it is convenient, see [4,5], to introduce another parameter,  $\alpha$  so that at  $\alpha = 1$  the neck radius is zero for any value of all other deformation parameters  $\alpha_n$ ,

$$\varepsilon = \frac{\alpha - 1}{4} \left[ \left( 1 + \sum_n \alpha_n \right)^2 + \left( 1 + \sum_n (-1)^n \alpha_n \right)^2 \right] + \frac{\alpha + 1}{2} \left[ 1 + \sum_n (-1)^n \alpha_{2n} (2n - 1)!! / (2^n n!) \right]^2. \quad (4)$$

It was demonstrated [6] that even a one-dimensional family of Cassinian shapes,  $\{\alpha = 0.98, \alpha_1\}$  is very close to the scission shapes of lowest liquid drop energy [7].

In the present study we take into account  $\alpha, \alpha_1, \alpha_2, \alpha_3$  and  $\alpha_4$  deformation parameters. With this shape parameterization we calculate the potential energy of deformation using the microscopic - macroscopic approach [8]:

$$E_{def}(\text{shape}) = E_{def}^{LD}(\text{shape}) + \delta E(\text{shape}), \quad (5)$$

with

$$\delta E = \sum_{n,p} [\delta E_{shell}^{(n,p)} + \delta E_{pair}^{(n,p)}]. \quad (6)$$

The summation in (6) is carried out over the protons ( $p$ ) and neutrons ( $n$ ). The  $E_{def}^{LD}$  in (5) is the macroscopic liquid-drop energy and  $\delta E$  contains the microscopic shell and pairing corrections calculated with the Woods-Saxon potential [4] for the given shape.

### 3. The mass and energy distributions of fission fragments

Keeping  $\alpha$  fixed at few values  $\alpha = 0.92, 0.94, 0.96, 0.98$  we have calculated the potential energy (5)–(6) as a function of shape parameters  $\alpha_1, \alpha_2, \alpha_3$  and  $\alpha_4$ .

In order to visualize the four-dimensional potential energy surface it was “projected” onto the two deformation parameters which have a physical meaning - the mass

asymmetry  $\delta$  and the elongation  $R_{12}$  which is defined as the distance between left and right parts of the nucleus.

For this, keeping  $\alpha, \alpha_2, \alpha_3$  and  $\alpha_4$  fixed the dependence of  $E_{def}$  on  $\alpha_1$  was transformed (by interpolation) into the dependence of  $E_{def}$  on  $\delta$ . Next, for each fixed value of  $\alpha_2, \alpha_3$  the dependence of  $E_{def}(\alpha, \delta, \alpha_2, \alpha_3, \alpha_4)$  was transformed into  $E_{def}(\alpha, \delta, \alpha_2, \alpha_3, R_{12})$  by the same method. Then, the deformation energy  $E_{def}(\alpha, \delta, \alpha_2, \alpha_3, R_{12})$  was minimized with respect to  $\alpha_2, \alpha_3$  keeping fixed  $\alpha, \delta, R_{12}$ . The resulting potential energy surface  $E_{def}(\alpha, \delta, R_{12})$  of  $^{236}\text{U}$  is shown in Fig. 1 as a function of mass asymmetry  $\delta$  and elongation  $R_{12}$  for a few fixed values of  $\alpha$ .

In Fig. 1 one can see the valleys leading to the mass asymmetric splitting of  $^{236}\text{U}$ . The mass asymmetry depends slightly on the value of the deformation parameter  $\alpha$ . The best agreement with experimental data one gets in case  $\alpha = 0.92$ . So, all the results below, both for  $^{236}\text{U}$  and  $^{252}\text{Cf}$ , were calculated with  $\alpha = 0.92$ .

One assumes that each point on the deformation-energy surface is populated with a probability given by the Boltzmann distribution,

$$P(\delta_i, q_i) = e^{-(E_{def}(\delta_i, q_i) - F)/T_{coll}}, \quad F \equiv -T_{coll} \log \sum_i e^{-E_{def}(\delta_i, q_i)/T_{coll}}. \quad (7)$$

Here  $T_{coll}$  is a parameter characterizing the width of the distribution (7) in the space of the deformation parameters.  $E_{def}(\delta_i, q_i)$  in (7) is the deformation energy (5). The  $\delta_i$  here is the mass asymmetry and  $q_i$  are the rest of deformation parameters,  $\alpha_2, \alpha_3, \alpha_4$ .

The distribution (7) is a basic assumption of any scission-point model. Its parameters were fitted in [2] so as to reproduce the experimental data.  $T_{coll}$  was found to be close to 1 MeV. In the pre-scission calculations shown below we use a somewhat larger value,  $T_{coll} = (1.5 \div 2.5)$  MeV.

The normalized mass distribution of the fission fragments  $Y(\delta)$  can be expressed then in terms of the probability (7) as,

$$Y(\delta) = \sum_i P(\delta, q_i). \quad (8)$$

In (8) the summation is carried out over the set of deformation points  $q_i \equiv \{-0.5 \leq \alpha_2 \leq 0.5, -0.5 \leq \alpha_3 \leq 0.5, -0.5 \leq \alpha_4 \leq 0.5\}$ .

The comparison of the experimental fission-fragment mass distributions for  $^{236}\text{U}$  [9] and  $^{252}\text{Cf}$  [10] and calculated values is shown in the top part of Fig. 2. As one can see, the experimental and calculated results are rather close to each other.

For the total kinetic energy distributions we use the same potential energy surface. For each shape defined by  $\alpha = 0.92, \alpha_1, \alpha_2, \alpha_3, \alpha_4$  one calculates the distance  $R_{12}$  between the centers of mass of left and right parts of the nucleus. The nucleus is supposed to be divided in two parts by the neck position. Then one estimates, in the point-charge approximation, the Coulomb interaction of the light (L) and heavy (H) fragments supposing uniform charge densities  $Z_L/Z_H = A_F^L/A_F^H$ .

$$E_{coul}^{int} = e^2 Z_L Z_H / R_{12} = TKE, \quad (9)$$

i.e. we neglect the kinetic energy in the fission direction at the scission point.

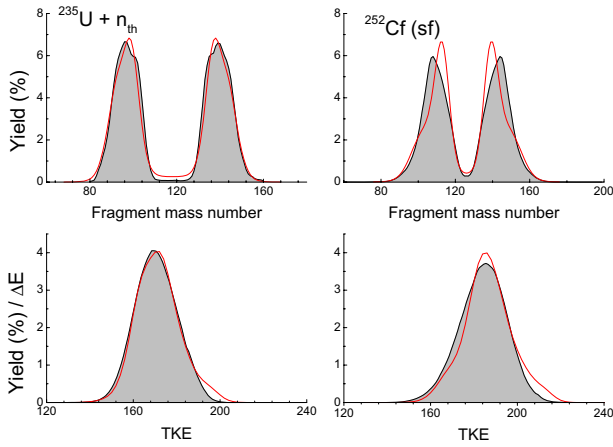


**Figure 2.** The comparison of experimental fission-fragment mass- and energy-distributions for  $^{236}\text{U}$  [9] and  $^{252}\text{Cf}$  [10] and calculated values (8)–(10) (red),  $T_{\text{coll}} = 1.5 \text{ MeV}$ ,  $\Delta E = 5 \text{ MeV}$ ,  $r_0 = 1.25 \text{ fm}$ .

The distribution is obtained using the formula:

$$Y(TKE) = \frac{1}{\sqrt{\pi} \Delta E} \sum_i P(\delta_i, q_i) e^{-\left(\frac{TKE(\delta_i, q_i) - TKE}{\Delta E}\right)^2}. \quad (10)$$

that accounts for the finite energy resolution through the parameter  $\Delta E$ .  $P(\delta_i, q_i)$  are the Boltzmann factors given by Eq. (7). The comparison of experimental and calculated results for  $Y(TKE)$  is shown in the bottom part of Fig. 2.

For both distributions (mass and TKE) a quite good agreement with recent experimental data [10] is obtained.

The weak point of this method - the value of the main elongation parameter  $\alpha = 0.92$  was chosen referring to the existing experimental data. In the next section an alternative definition of the nuclear shapes at the scission point is considered which defines the scission point in quite a formal way.

#### 4. The optimal scission shapes

The optimal shape approach [7] allows for the definition of the shape of the fissioning nucleus without imposing any shape parametrization. For the left-right and axially symmetric nucleus it defines the profile function  $\rho(z)$  by looking for the minimum of the liquid-drop energy,  $E_{\text{LD}} = E_{\text{surf}} + E_{\text{Coul}}$  under the constraint that the volume  $V$  and the elongation  $R_{12}$  are fixed,

$$\frac{\delta}{\delta \rho} (E_{\text{LD}} - \lambda_1 V - \lambda_2 R_{12}) = 0. \quad (11)$$

The deformation parameter  $R_{12}$  was chosen in [7] as the distance between the centers of mass of the left and right parts of the nucleus,

$$R_{12} = \frac{2\pi}{V} \int_{z_1}^{z_2} \rho^2(z) |z| dz, \quad V = \pi \int_{z_1}^{z_2} \rho^2(z) dz. \quad (12)$$

The variation in (11) leads to an integro-differential equation for  $\rho(z)$

$$\rho \rho'' = 1 + (\rho')^2 - \rho [\lambda_1 + \lambda_2 |z| - 10 x_{\text{LD}} \Phi_S] [1 + (\rho')^2]^{\frac{3}{2}}. \quad (13)$$

Here  $\Phi_S \equiv \Phi(z, \rho(z))$  is the Coulomb potential at the nuclear surface and  $x_{\text{LD}}$  is the fissility parameter of the liquid drop.

By solving Eq. (13) for given  $\lambda_2$  ( $\lambda_1$  is fixed by the volume conservation condition) one obtains the sequence of profile functions  $\rho(z)$ . Varying the parameter  $\lambda_2$  from some minimal to maximal value, one obtains the shapes ranging from a very oblate shape (disk) up to the two touching spheres. The solutions of Eq. (13) describe the shapes that correspond to the *smallest* liquid drop energy for given elongation  $R_{12}$ .

For each  $\rho(z)$  one can easily calculate (numerically) the deformation  $R_{12}$  and other quantities of interest like Coulomb or surface energies and plot the deformation energy  $E_{\text{def}} = E_{\text{LD}} - E_{\text{LD}}^{(0)}$  as a function of the elongation  $R_{12}$ . It turns out, see [7], that the elongation  $R_{12}$  of these shapes is limited by some maximal value  $R_{12}^{(\text{crit})}$ . For  $R_{12} > R_{12}^{(\text{crit})}$  the compact solutions of Eq. (13) do not exist. For  $R_{12} > R_{12}^{(\text{crit})}$  the solutions of (13) represent the two separated fragments. This critical deformation  $R_{12}^{(\text{crit})}$  was interpreted in [7] as the scission point. Note, that  $R_{12}^{(\text{crit})}$  depends only on the fissility parameter  $x_{\text{LD}}$ . So, for any given nucleus the  $R_{12}^{(\text{crit})}$  is defined completely unambiguously.

For the description of the fission process the optimal shape approach of [7] should be generalized to the reflection-asymmetric shapes. For this aim one has to include into Eq. (11) another constraint that fixes the mass asymmetry of the drop.

In [12] it was suggested to replace the conventional definition of the mass asymmetry  $\delta$  and elongation  $R_{12}$  by

$$\tilde{R}_{12} = \frac{\pi}{V} \int_{z_1}^{z_2} f_2(z) \rho^2(z) dz, \quad \tilde{\delta} = \frac{\pi}{V} \int_{z_1}^{z_2} f_3(z) \rho^2(z) dz, \quad (14)$$

$$f_2 = \sqrt{(z - z^*)^2 + (\Delta z)^2}, \quad f_3 = \frac{(z - z^*)}{\sqrt{(z - z^*)^2 + (\Delta z)^2}}. \quad (15)$$

In the case that the nuclear shape has a neck,  $z^*$  coincides with the position of the neck,  $z^* = z_{\text{neck}}$ . In the calculations reported below  $\Delta z$  was chosen as in [12],  $\Delta z = 0.25 R_0$ .

However, this turned out not to be enough. The shape of the fissioning nuclei is defined not only by the liquid drop part of the deformation energy but also by the shell effects. It was shown in [4] that due to the shell structure in the deformation energy of actinide nuclei there exists a deep minimum corresponding to the shape at which one part is almost spherical due to the large shell correction of the double magic fragment  $^{132}\text{Sn}$  and another part is very elongated. Clearly, such a shape can not be obtained within the variational approach (11) where the deformation of the fragments is completely fixed by the deformation dependence of the liquid-drop energy.

In order to account for the influence of shell effects on the shape of the fissioning nucleus it is necessary to include into the optimal shapes more degrees of freedom. For this purpose in the present work we include in the variational procedure (13) another constraint of the form  $-\lambda_5 Q_3$

$$\frac{\delta}{\delta \rho} [E_{\text{LD}} - \lambda_1 V - \lambda_2 \tilde{R}_{12} - \lambda_3 \tilde{\delta} - \lambda_5 Q_3] = 0, \quad (16)$$

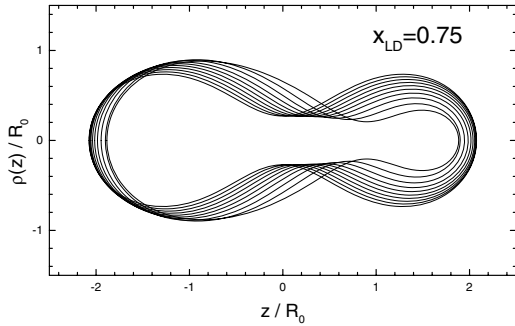


**Figure 3.** Solutions of Eq. (16) with  $\lambda_5 = 0$  at the maximal elongation  $R_{12}^{(crit)}$  for different values of the mass asymmetry  $\delta = 0, 0.1, \dots, 0.6$ .

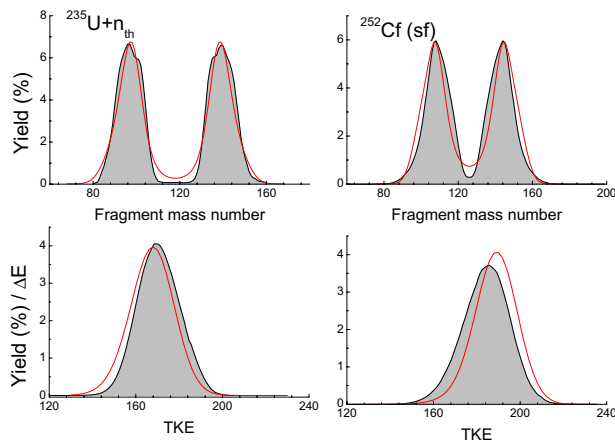


**Figure 4.** The comparison of experimental fission-fragment mass- and energy-distributions for  $^{236}\text{U}$  [9] and  $^{252}\text{Cf}$  [10] and values (8)–(10) (red) calculated with optimal shapes,  $T_{coll} = 2.5$  MeV,  $\Delta E = 13$  MeV,  $r_0 = 1.25$  fm.

where  $Q_3$  is the octupole moment relative to the position of the neck. Depending on the sign and the magnitude of  $\lambda_5$  the account of  $\lambda_5 Q_3$  in (16) allows to make one part of shape more spherical and another - more elongated. Equation (16) can be solved in the same way as Eq. (13). Some examples of the shapes at the scission point  $R_{12}^{(crit)}$  (maximal possible value of  $R_{12}$  at fixed  $\lambda_3$ ) for a few values of the mass asymmetry  $\delta$  are shown in Fig. 3.

The solutions of (16) at  $R_{12} = R_{12}^{(crit)}$  depend now not only on the mass asymmetry  $\delta$  but also on the value of the Lagrange multiplier  $\lambda_5$ . The value of  $\lambda_5$  eventually was fixed by the minimization of the total deformation energy (liquid drop plus shell correction) with respect to variation of  $\lambda_5$ . The region of variation of  $\lambda_5$  is chosen

so that it contains the minimum of the total deformation energy.

The deformation energy calculated with the solutions of Eq. (16) (we call them optimal shapes) was used then in expressions (7), (8) and (10) to find the mass and energy distributions of the fission fragments

The comparison of the experimental fission-fragment mass- and energy-distributions for  $^{236}\text{U}$  [9] and  $^{252}\text{Cf}$  [10] and calculated values (8)–(10) is shown in Fig. 4. As one can see, the agreement is rather good. Since the calculations were done with the minimum number of constraints one can consider these results encouraging.

## 5. Summary

We have defined the scission point shape by two methods: by the Cassini shape parameterization and by the optimal shape method. The deformation energy at the scission point was used in order to calculate the fission-fragment mass- and the total kinetic energy-distributions for  $^{235}\text{U}(n, f)$  and  $^{252}\text{Cf}(sf)$  reactions within an improved scission point model. In both cases we have found out that the calculated results are very close to the existing experimental data.

This work was supported in part by EC EURATOM FP7 project CHANDA.

## References

- [1] M. Rizea, N. Carjan, Nucl. Phys. A **909**, 50 (2013)
- [2] B.D. Wilkins, E.P. Steinberg, R.R. Chasman, Phys. Rev. C **14**, 1832 (1976)
- [3] N. Carjan, F.A. Ivanyuk, Yu. Oganessian, G. Ter-Akopian, Nucl. Phys. A **942**, 97 (2015)
- [4] V. Pashkevich, Nucl. Phys. A **169**, 275 (1971)
- [5] V. Pashkevich, Nucl. Phys. A **477**, 1 (1988)
- [6] N. Carjan, F. Ivanyuk, V. Pashkevich, Physics Procedia **31**, 66 (2012)
- [7] V.M. Strutinsky, N.Ya. Lyashchenko, N.A. Popov, Nucl. Phys. **46**, 659 (1963)
- [8] M. Brack, J. Damgaard, A.S. Jensen, H.C. Pauli, V.M. Strutinsky, C.Y. Wong, Rev. Mod. Phys. **44**, 320 (1972)
- [9] A. Göök, F.-J. Hamsch, W. Gertz, M. Vidali private communication
- [10] A. Göök, F.-J. Hamsch, M. Vidali, Phys. Rev. C **90**, 064611 (2014)
- [11] F.A. Ivanyuk, K. Pomorski, Phys. Rev. C **79**, 054327 (2009)
- [12] F.A. Ivanyuk, Physics Procedia **47**, 17 (2013)